Numerical simulation of a two-dimensional S-shaped inlet

Numerical simulation of a two-dimensional S-shaped inlet

Haoran Zhan[1*]

[1] Key Laboratory of Aircraft Environment Control and Life Support, MIIT, Nanjing University of Aeronautics and Astronautics, Nanjing 210016, China

[*]Corresponding author's e-mail: haoranzhan@nuaa.edu.cn

Abstract. In order to solve the problem that different operation conditions affect the performance of S-shaped inlet, we have carried out a numerical study on a two-dimensional S-shaped inlet and analysed the influences of incoming Mach number, attack of angle α and the outlet pressure on the performance parameters of the inlet, such as the total pressure recovery coefficient, total compression ratio and the steady-state total pressure distortion index at the exit of inlet. The results show that Ma number and the outlet pressure are the main factors affecting inlet performance. With the increase of Ma number, the total pressure recovery coefficient of inlet decreases from 0.975 to 0.793, the total compression ratio decreases from 1.212 to 1.146, and the steady-state total pressure distortion index increases from 0.0536 to 0.377. The flow energy loss in the inlet increases, the flow uniformity decreases, and the inlet performance becomes worse. With the increase of the outlet pressure, the total pressure recovery coefficient of inlet rises from 0.875 to 0.931, the total compression ratio rises from 1.101 to 1.216, and the steady-state total pressure distortion index decreases from 0.219 to 0.123. The mass flow rate of inlet and airflow loss decrease, and the performance of the inlet improves. We study the influence of different operation conditions on the inlet performance, which provides a certain reference for the performance evaluation of S-shaped inlet.

1. Introduction

As an important part of the propulsion system, the inlet is mainly used to capture, compress and rectify the air flow to provide high-quality air flow for the engine[1]. The traditional inlet has a bad stealth ability and lower total pressure recovery coefficient, having a fatal damage to the engine[2]. S-shaped inlet is widely used in the propulsion system of modern military aircraft due to its compact structure, good stealth ability and easy maintenance. For example, American F-22 fighter jets and Predator C adopt S-shaped inlet[3][4][5].

Up to now, scholars around the world have carried out a lot of studies on the flow characteristics of S-shaped inlet. Kirk et al. [6] carried out numerical and experimental studies on a serpentine inlet using self-programmed programs, explaining the flow separation and secondary flow phenomena in the inlet, and the numerical calculation results are in good agreement with the experimental results, indicating the feasibility of the numerical method. Nima et al. [7]used numerical simulation to study the S-shaped inlet used on a certain UAV, and discussed the influence of sideslip angle of the inlet on the inlet's working performance, and the results showed that the sideslip angle had a weak influence on the inlet. Zhang et al. [8]analyzed the mechanism of swirl distortion in S-shaped inlet by means of numerical simulation, and proposed a swirl evaluation index.

In this paper, we take a two-dimensional S-shaped inlet as the research object to analyze the internal and external flow fields of the inlet under different working conditions, aiming to explore the effects of

Ma number, angle of attack α and the outlet pressure on the inlet performance, providing reference for the inlet flow control design.

2. The Computational model and numerical method

The S-duct inlet flow is a typical compressible problem[9], the governing equation can be written in the following form:

$$\frac{\partial \rho}{\partial t}+\frac{\partial u_i}{\partial x_i}=0 \tag{1}$$

$$\frac{\partial(\rho u_i)}{\partial t}+\frac{\partial(\rho u_i u_j)}{\partial x_j}=-\frac{\partial p}{\partial x_i}+\frac{\partial \tau_{ij}}{\partial x_j} \tag{2}$$

$$\frac{\partial(\rho E)}{\partial t}+\frac{\partial[(\rho E+p)u_i]}{\partial x_i}=-\frac{\partial q_i}{\partial x_i}+\frac{\partial(u_j \tau_{ij})}{\partial x_i} \tag{3}$$

Where ρ is the fluid density, u_i the velocity components, p the pressure, E the total energy, q the heat flux, t the time, τ_{ij} the shear stress.

The geometric model and mesh division of the two dimensional S-duct inlet studied in this paper are shown in the Figure 1. The computational domain consists of an outflow field and an inlet flow field. The outflow field is composed of a 40m*40m rectangle. In order to reduce the influence of the internal flow filed on the outlet of the S-duct inlet, we extent the outlet of the inlet a bit. The calculation conditions are as follows: the flight height H=5.5 km, static pressure P=50539Pa, static temperature T=252.4k. The computational grid adopts structured grid, and the total number of grid is about 50,000. We choose $k-\omega$ SST model as turbulent model, using the Density-Based solver and $y^+ \approx 1$. The ideal-gas is selected for fluid. In terms of setting the boundary conditions, the boundary of the outflow field is Pressure-far-field and the outlet of the S-duct inlet is Pressure-Outlet.

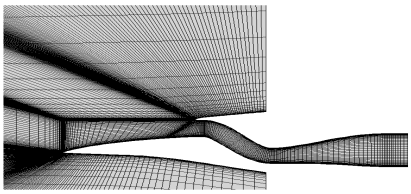

Figure 1. The geometric model and mesh

3. Results and discussion

In order to evaluate the performance of the inlet, the total pressure recovery coefficient (TPR), the total compression ratio (π) and the steady-state total pressure distortion index ($\overline{D}$) are used to measure. In general, the inlet is required to have a higher TPR and a lower distortion index [10].

The TPR is defined as the ratio of the total outlet pressure of the inlet to the total free flow pressure, which is used to measure the energy loss degree of the flow. Its expression is as follows:

$$TPR=\frac{P_2^*}{P_\infty^*} \tag{4}$$

Where P_2^* is the total outlet pressure of the inlet, P_∞^* the total pressure of free flow.

π is defined as the ratio of the average static pressure at the exit of inlet to the static pressure of free flow, which is used to measure the expansion capacity of the inlet. Its expression is as follows:

$$\pi=\frac{\overline{P_2}}{P_\infty} \tag{5}$$

Where $\overline{P_2}$ is the average static pressure at the exit of inlet, P_∞ the static pressure of free flow.

The $\overline{D}$ is defined as the ratio of the difference between the maximum total pressure and minimum total pressure and the average total pressure at the outlet section of the inlet, which is used to measure the total pressure unevenness at the outlet section. Its expression is as follows:

$$\overline{D} = \frac{P_{\max}^{*} - P_{\min}^{*}}{\overline{P^{*}}} \tag{6}$$

Where $P_{\max}^{*}$ is the maximum total pressure of exit of inlet, $P_{\min}^{*}$ is the minimum total pressure of exit of inlet, $\overline{P^{*}}$ is the average total pressure of exit of inlet.

3.1. The influence of Ma number on inlet

In order to study the different Ma numbers influence on the performance of the inlet, figure 2.shows the curve of inlet performance versus Ma number. When Ma = 0.6~0.9, with the increase of Ma number, the TPR and the total compression ratio at exit of inlet decrease and the steady-state total pressure distortion index increases gradually. It shows that the performance of the inlet becomes worse with the increase of Ma number.

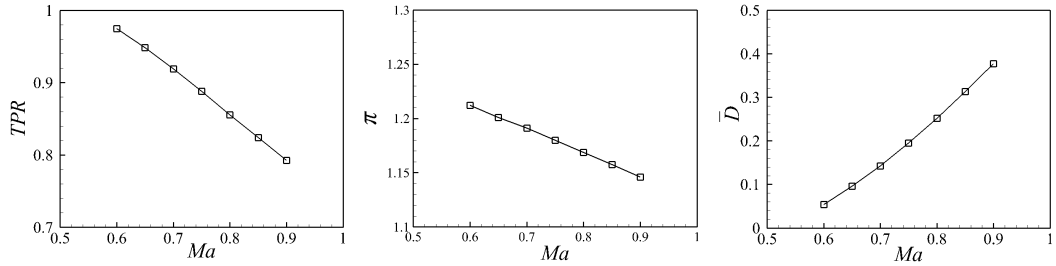

Figure 2. The curve of inlet performance versus *Ma*

In order to further analyse the flow Ma number effect on the performance of inlet, figure 3.shows contours of the total pressure distribution of the two-dimensional inlet at different Ma numbers. It can be seen from contours that the total pressure of outfield basically remains the same. Total pressure losses when entering the inlet. The larger Ma number is, the more serious airflow loss is, leading to the TPR decreases with the increase of Ma number.

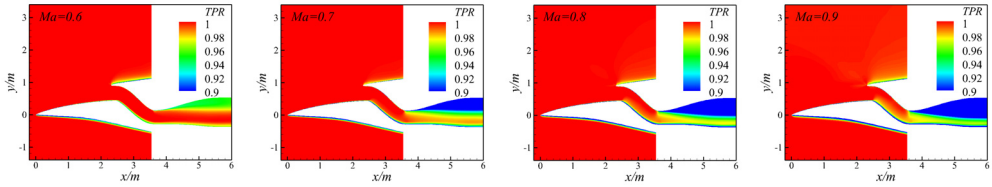

Figure 3. Contour of total pressure distribution under different Ma numbers

Figure 4.shows contours of pressure distribution and streamlines under different Ma numbers. It can be seen from the figure that when Ma number is small, flow separation is relatively small, and the larger Ma number is, the larger flow separation is, which leads to the increase of the steady-state total pressure distortion index at the outlet with the increase of Ma number. Due to the S-shaped configuration of the inlet, a low pressure area is formed in the lower part of the first bend and the upper part of the second bend. Under the condition of a given outlet pressure, the static pressure at the outlet of the inlet decreases with the increase of Ma number, resulting in a decrease in the compression ratio with the increase of Ma number.

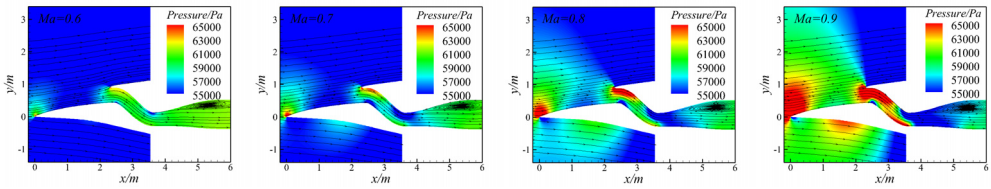

Figure 4. Contours of static pressure distribution and streamlines under different Ma numbers

3.2. The influence of attack of angel α on inlet

In order to study the influence of incoming flow angle of attack α on inlet performance, figure 5.shows the curve of inlet performance versus *α* when Ma= 0.8. It can be seen that, when Ma number is constant, TPR changes little in the range of negative angle of attack α, and in the range of positive α, the TPR decreases. For the total compression ratio, when the angle of attack α is less than 10°, the total compression ratio basically remains unchanged, and when the angle of attack α is 10°, the total compression ratio increases suddenly. For the steady-state total pressure distortion index, it increases firstly and then decreases with the increase of the angle of attack α.

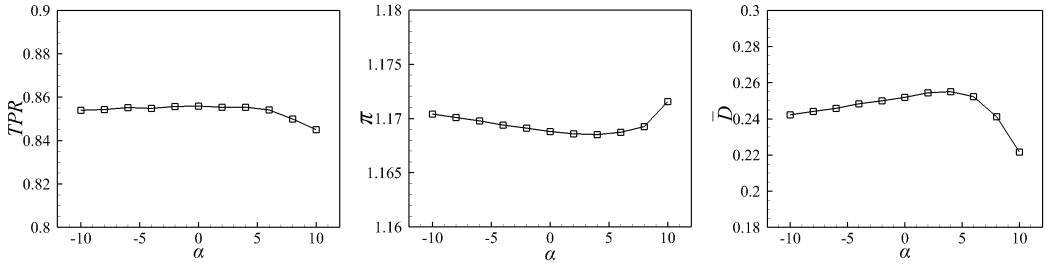

Figure 5. The curve of inlet performance versus *α*

In order to further analyse the influence of angle of attack α on inlet performance, we study the inlet fluid field at α=0°, -10° and 10° when Ma = 0.8. Figure 6.shows contours of total distribution under different angle of attack α. We can know that the angle of attack α has little influence on the TPR. When α=10°, the air flow at the inlet loses, leading to a slight decrease on the TPR at the outlet. In the range of negative α, the TPR basically remains unchanged.

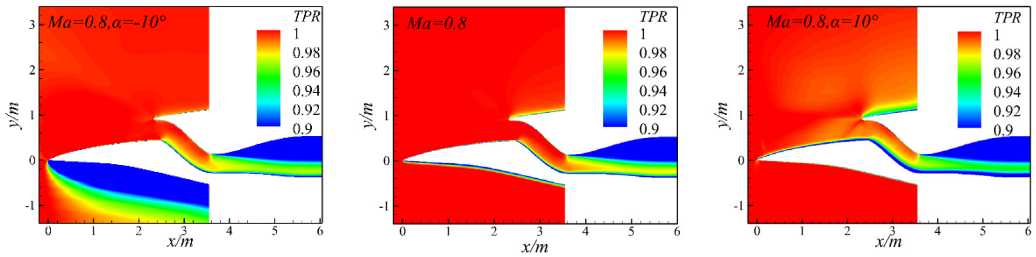

Figure 6. Contours of total pressure distribution under different α

Figure 7.shows contours of static pressure distribution and streamlines under different α. It can be seen that the fuselage has a downward sloping angle, causing airflow smoothly going into the inlet. And the inlet forms a low pressure area at the lower part of the first turn and the upper part of the second turn, and the static pressure distribution changes little at the exit, thus the total compression ratio of the exit of the inlet is less affected by the α.

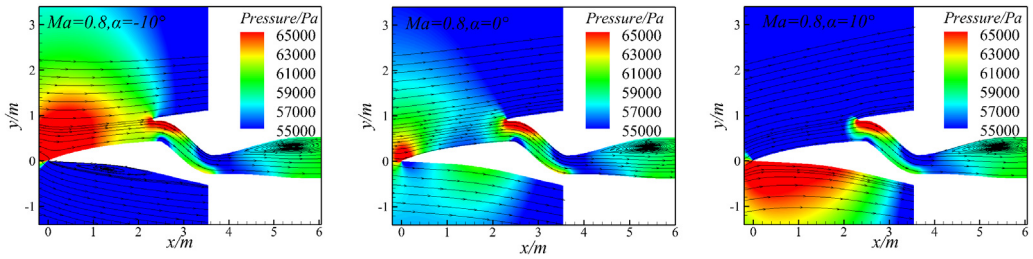

Figure 7. Contours of static pressure distribution and streamlines under different α

3.3. The influence of outlet pressure on inlet

In order to study the influence of inlet outlet pressure on inlet performance, figure 8.shows the curve of inlet performance versus outlet pressure at different Ma numbers. As can be seen from the figure, when the Ma number of incoming flow is constant, with the increase of outlet pressure, the inlet performance becomes better, the TPR and total compression ratio rise linearly, and the steady-state total pressure distortion index decreases linearly. The change law is basically consistent under different Ma numbers of incoming flow.

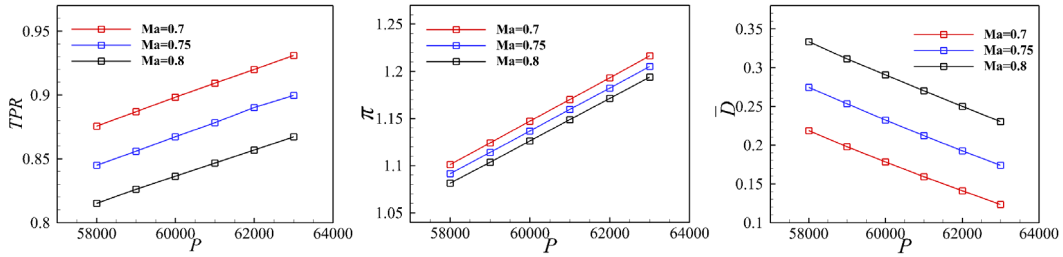

Figure 8. The curve of inlet performance versus *outlet pressure*

In order to further analyse the influence of outlet pressure on the inlet performance, conclusions can be drawn by analysing the inlet flow field structure. Since the variation rules of inlet performance are basically the same, the inlet flow field under different pressures was analysed when Ma=0.7. Figure 9. shows the contours of total distribution under different outlet pressure. It can be seen from the figure 9.that the low pressure area above the inlet outlet decreases with the increase of outlet pressure, so the total pressure recovery coefficient increases with the increase of outlet pressure.

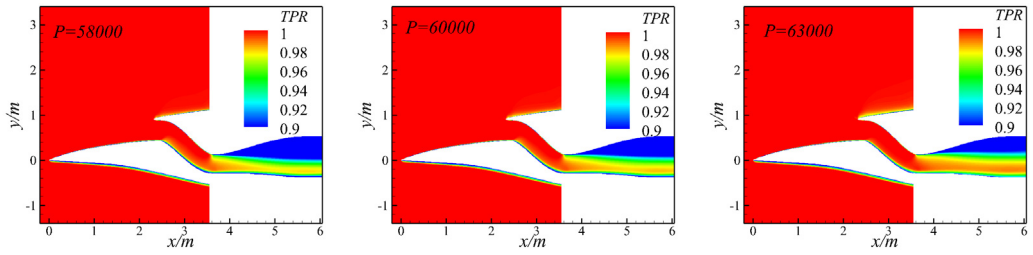

Figure 9. Contours of total pressure distribution under different outlet pressure

Figure 10.shows contours of static pressure distribution and streamlines under different outlet pressure. It can be seen from the figure that with the increase of outlet pressure, the inlet outlet static pressure increases, the total compression ratio increases and the flow separation intensity weakens. The inlet total pressure distortion index decreases, and the inlet operating performance becomes better.

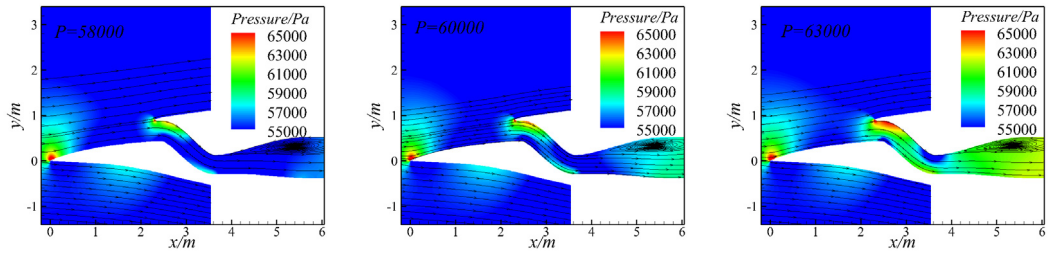

Figure 10. Contours of static pressure distribution and streamlines under different outlet pressure

4. Conclusion

In this article, we have studied a two-dimensional S-shaped inlet by numerical simulation and analysed the variation characteristics of inlet performance parameters under different operation conditions. The results show that:

1) The performance of S-shaped inlet is greatly affected by Ma number and outlet pressure, but less affected by angle of attack α. Under the condition that the angle of attack α and outlet pressure remain unchanged, with the increase of Ma, the TPR and the total compression ratio at the exit of the inlet decrease, the steady-state total pressure distortion index increases, and the inlet performance deteriorates.
2) Under certain incoming flow conditions, the TPR of the inlet increases with the increase of outlet pressure, and the steady-state total pressure distortion index decreases, which make inlet performance become better.
3) Angle of attack α is not the main factor affecting the inlet performance and is less affected by the angle of attack α.

References

[1] An J N. Study of influence of geometry parameters on aerodynamic characteristics of S-duct inlet. (2020) Aeroengine. 46(02): 51-55.
[2] Gerolymos G A, Joly S, Mallet M, et al. Reynolds-stress model flow prediction in aircraft engine intake double S-shaped duct. (2010) Journal of Aircraft. 47(4): 1368-1381.
[3] Guo R W, Seddon J. The Swirl in a S-Duct of Typical Air Intake Proportions.(1983) Aeronautical Quarterly, 34: 99-129.
[4] Hall D K, Huang A C, Uranga A, et al. Boundary Layer Ingestion Propulsion Benefit for Transport Aircraft. (2017) Journal of Propulsion and Power. 33(5): 1118-1129.
[5] Tanguy G, Macmanus D G, Zachos P K, et al. Passive Flow Control Study in an S-Duct Using Stereo Particle Image Velocimetry. (2017)AIAA Journal. 55(6): 1862-1877.
[6] Kirk A M, Gargoloff J I, Rediniotis O K, et al. Numerical and experimental investigation of a serpentine inlet duct. (2009) International Journal of Computational Fluid Dynamics. 23(3):245–258.
[7] Nima Shojaee S M, Hazaveh H A. Investigation of total pressure distribution at aerodynamic interface plane of an “S-shaped” air intake at sideslip condition. (2012)International Journal of Natural and Engineering Sciences. 6(3): 87-94.
[8] Zhang X F, Jiang J, Fu X G. Numerical simulation and characteristic analysis of swirl distortion in S-duct inlet. (2012) Gas Turbine Experiment and Research. 25(03): 31-35+48.
[9] Sun S, Tan H J. Flow Characteristics of an Ultracompact Serpentine Inlet with an Internal Bump. (2018) Journal of Aerospace Engineering. 31(2)
[10] Simpson R L . Junction Flows. (2001) Annual Review of Flu‐ id Mechanics. 33: 415-443.